Please cite this article in press as: Jepson et al., High-Fidelity Reproduction of Spatiotemporal Visual Signals for Retinal Prosthesis, Neuron (2014), http://dx.doi.org/10.1016/j.neuron.2014.04.044

Neuron
Report

High-Fidelity Reproduction of Spatiotemporal Visual Signals for Retinal Prosthesis

Lauren H. Jepson,[1,2] Pawel Hottowy,[3] Geoffrey A. Weiner,[4] Władysław Dabrowski,[3] Alan M. Litke,[5] and E.J. Chichilnisky[1,6,*]
[1]Systems Neurobiology Laboratories, Salk Institute for Biological Studies, La Jolla, CA 92037, USA
[2]Bioengineering Department, University of California, San Diego, La Jolla, CA 92093, USA
[3]AGH University of Science and Technology, Faculty of Physics and Applied Computer Science, 30-059 Krakow, Poland
[4]Neuroscience Graduate Program, University of California, La Jolla, CA 92093, USA
[5]Santa Cruz Institute for Particle Physics, University of California, Santa Cruz, Santa Cruz, CA 95064, USA
[6]Department of Neurosurgery and Hansen Experimental Physics Laboratory, Stanford University, Stanford, CA 94305, USA
*Correspondence: ej@stanford.edu
http://dx.doi.org/10.1016/j.neuron.2014.04.044

SUMMARY

Natural vision relies on spatiotemporal patterns of electrical activity in the retina. We investigated the feasibility of veridically reproducing such patterns with epiretinal prostheses. Multielectrode recordings and visual and electrical stimulation were performed on populations of identified ganglion cells in isolated peripheral primate retina. Electrical stimulation patterns were designed to reproduce recorded waves of activity elicited by a moving visual stimulus. Electrical responses in populations of ON parasol cells exhibited high spatial and temporal precision, matching or exceeding the precision of visual responses measured in the same cells. Computational readout of electrical and visual responses produced similar estimates of stimulus speed, confirming the fidelity of electrical stimulation for biologically relevant visual signals. These results suggest the possibility of producing rich spatiotemporal patterns of retinal activity with a prosthesis and that temporal multiplexing may aid in reproducing the neural code of the retina.

INTRODUCTION

Retinal prostheses are designed to restore visual function to patients blinded by photoreceptor disease, by electrically stimulating surviving cells in a manner that conveys useful visual signals to the brain (for review, see Shepherd et al., 2013). Although present-day prostheses produce only limited visual function (Dorn et al., 2013; G. Richard et al., 2008, ARVO abstract; Klauke et al., 2011; Barry and Dagnelie, 2012; Humayun et al., 2012; da Cruz et al., 2013), experiments in isolated retina have demonstrated the capacity to electrically stimulate individual retinal ganglion cells (RGCs) to fire individual spikes (Jensen et al., 2005; Fried et al., 2006) with high spatial and temporal precision (Fried et al., 2006; Sekirnjak et al., 2006; Sekirnjak et al., 2008; Hottowy et al., 2012; Jepson et al., 2013). These findings raise the possibility of faithful reproduction of the neural code of the retina, and thus much more acute artificial vision, with future prostheses (see Jensen et al., 2009; Fried et al., 2006; Ryu et al., 2011). However, it is well known that naturalistic visual experience relies not on the activity of any individual RGC but on diverse spatiotemporal patterns of activity in multiple distinct populations of RGCs. Thus, a central problem in producing high-resolution prostheses is to faithfully recreate spatiotemporal patterns of population activity in the output of the retina (Nirenberg and Pandarinath, 2012; Hottowy et al., 2012). Importantly, because different visual signals are conveyed to different targets in the brain by roughly 20 distinct types of retinal ganglion cells (see Dacey, 2004), a faithful reproduction of the retinal output must also respect the functional role of different cell types, particularly those that are likely to play an important role in human vision.

A simple and behaviorally significant example is the pattern of activity produced by moving objects, an essential feature of biological vision. Visual motion induces a traveling wave of activity in populations of RGCs (Chichilnisky and Kalmar, 2003; Frechette et al., 2005). In primates, these waves drive the activity of neurons in the brain, which are tuned to visual movement and are thought to mediate a variety of essential visual behaviors based on image motion. The dominant retinal signals subserving motion sensing in human and nonhuman primates are thought to be those present in the ON and OFF parasol RGC populations (Perry et al., 1984; Dacey and Petersen, 1992) (see Merigan and Maunsell, 1990), each of which uniformly tiles the retinal surface and conveys a complete rendition of the visual scene to the magnocellular visual pathway of the brain. Parasol cells, which comprise about 16% of the output of the primate retina (Dacey, 2004), have been shown to respond robustly and with high spatial and temporal precision to electrical stimulation (Sekirnjak et al., 2008; Jepson et al., 2013). Thus, a natural goal for the development of future high-precision retinal prostheses is to activate parasol cells in a manner that mimics responses to moving visual targets.

RESULTS

To test how faithfully retinal motion signals can be reproduced, we performed multielectrode recordings and electrical and

Please cite this article in press as: Jepson et al., High-Fidelity Reproduction of Spatiotemporal Visual Signals for Retinal Prosthesis, Neuron (2014), http://dx.doi.org/10.1016/j.neuron.2014.04.044

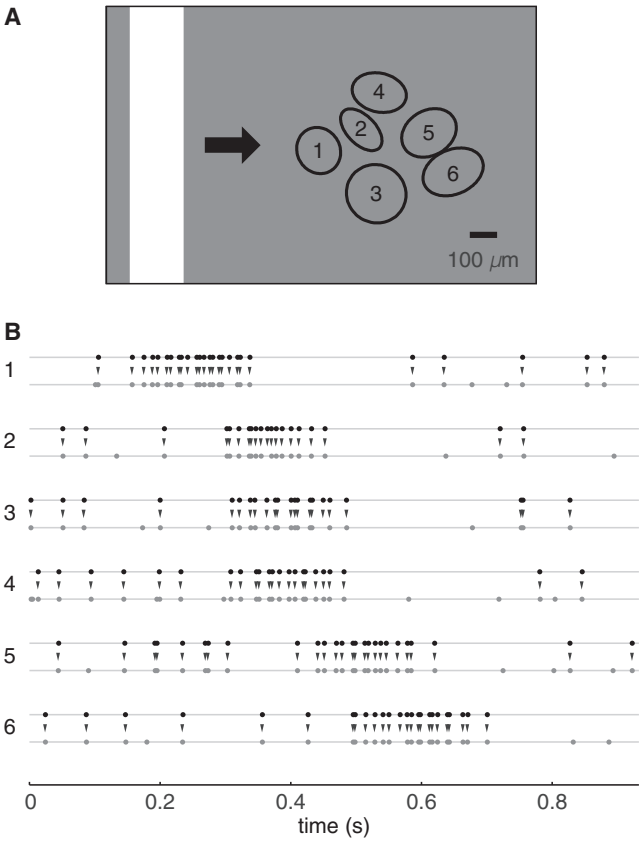

Figure 1. Spatiotemporal Visual and Electrical Activation of a Complete Local Population of Retinal Ganglion Cells

(A) Receptive fields of six ON parasol cells measured in a single recording are shown with ellipses representing the 1 SD contour of a Gaussian fit to the spatial sensitivity profile (see Experimental Procedures). Cell numbers relate to (B). Schematic of moving bar stimulus is shown at left. (B) For each cell, spikes recorded during a single trial of moving bar visual stimulation that was selected for subsequent replication are shown as black dots in the top traces. Times of applied current pulses, derived from the spikes recorded in response to visual stimulation, are shown as arrowheads in the middle traces. Times of spikes recorded during a single electrical stimulation trial are shown as gray dots in the bottom traces.

visual stimulation in isolated peripheral macaque monkey retina. First, RGC responses to visual stimulation were recorded and used to identify distinct cell types, each of which formed a mosaic with receptive fields uniformly tiling the region of retina recorded (Figure 1A) (Devries and Baylor, 1997; Chichilnisky and Kalmar, 2002). The ON and OFF parasol cell types were identified on the basis of their receptive field properties and density (Chichilnisky and Kalmar, 2002). Encoding of visual stimuli was then examined by presenting a moving white bar (Figure 1A) traveling at 6.7 deg/s across a gray photopic background. As expected from many studies, including previous studies with very similar stimulation and recording methods (Chichilnisky and Kalmar, 2003; Frechette et al., 2005), these stimuli induced activity sequentially in the ON parasol cells, according to the location of their receptive fields along the axis of motion (Figure 1B, black dots). The spatiotemporal pattern of spikes in the collection of ON parasol cells reflects the direction and speed of movement and is thought to be an essential component of motion sensing in primates.

To assess the potential to recreate the spatiotemporal activity patterns induced by visual motion, we selected individual electrodes and current amplitudes that would efficiently stimulate each of the recorded ON parasol cells, based on responses to pulses delivered independently through individual electrodes (Jepson et al., 2013) (see Experimental Procedures). Current pulses (Figure 1B, arrowheads) were then delivered at the times of the spikes recorded in a single trial of visual stimulation (Figure 1B, black dots), in an attempt to activate the cells in the correct pattern. The spikes elicited by electrical stimulation combined with the spikes attributable to ongoing background activity (Figure 1B, gray dots) produced a pattern of activity resembling the pattern evoked by the visual stimulus.

To quantify how accurately the neural code for visual motion was reproduced, we measured the variability of neural responses across trials, for both visual and electrical stimulation, in the same collection of identified RGCs. Moving visual stimuli elicited a reproducible pattern across trials (Figure 2A), similar to that seen in previous work in which the effective temporal resolution of the motion signal was ~10 ms (Chichilnisky and Kalmar, 2003; Frechette et al., 2005). Electrical stimulation, however, produced much more precise spike timing (Figure 2B, spikes precisely aligned across trials), with ~0.1 ms variability in the time of elicited spikes, consistent with previous studies (Fried et al., 2006; Sekirnjak et al., 2006; Sekirnjak et al., 2008; Hottowy et al., 2012; Jepson et al., 2013). These electrically elicited spikes were superimposed on more variable patterns of spontaneous activity (Figure 2B, spikes not aligned across trials). No unintended activation of nontargeted ON parasol cells was observed (Jepson et al., 2013; Sekirnjak et al., 2008), as evidenced by the lack of time locking of responses in different cells, while individual cells were highly time locked across trials. Also, consistent with previous findings (Jepson et al., 2013), minimal crosstalk was observed with OFF parasol cells examined in one preparation (the preparation of Figure 3B, right): of the six OFF parasol cells recorded and forming a local mosaic over the same region as the ON parasol cells, only one cell exhibited electrical activation, on less than 14% of trials (data not shown). Thus, electrical stimulation reproduced the essential spatiotemporal patterns of activity in the targeted population of cells, and the patterns were far more reproducible across trials than the patterns induced by visual stimulation. Note, however, that periods of reduced firing at certain phases of the visual stimulus (e.g., 0.7–0.9 s in the bottom raster of Figure 2A) were apparently not accurately reproduced in electrical stimulation (e.g., same cell and time range in Figure 2B). Some reduction in firing was observed, probably attributable to refractoriness after high-frequency firing (Sekirnjak et al., 2006).

To evaluate the fidelity of the behaviorally relevant visual signal produced by electrical stimulation, we used the spiking activity of the recorded cells to extract an estimate of stimulus speed. This was accomplished using a computational algorithm based on standard models of motion sensing in the central visual system (Adelson and Bergen, 1985; Simoncelli and Heeger, 1998; Chichilnisky and Kalmar, 2003; Frechette et al., 2005). The

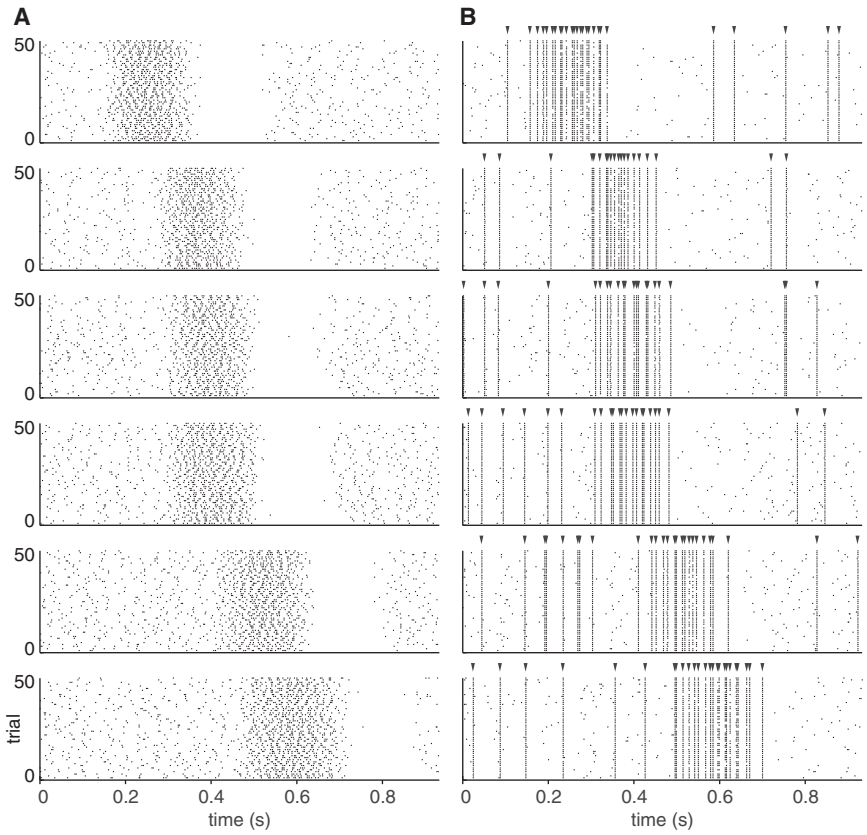

Figure 2. Responses to Repeated Presentations of Visual and Electrical Stimuli

(A) Spike trains elicited by a moving bar visual stimulus are shown for the same cells as in Figure 1, in raster format, with each tick representing the time of a spike, and each row representing a single trial. Coarse vertical band structure for each cell reveals reproducibility of visual responses across trials. (B) Spike trains obtained during electrical stimulation trials with no visual stimulus are shown in the same format as (A). Electrical stimuli (arrowheads above rasters) were delivered at the times of spikes recorded in a single visual stimulation trial (see Figure 1). Precise vertical band structure reflects electrically elicited spikes occurring at a reproducible time in many or all trials.

algorithm exploits the temporal sequence of activation of cells in each trial, by correlating spikes trains in space and time (Chichilnisky and Kalmar, 2003; Frechette et al., 2005). For each trial of visual stimulation, this computation produced a net motion signal as a function of putative speed (Figure 3A, black traces), which can be interpreted as the strength of evidence in the spike trains for motion at that speed. This function exhibited a clear peak near the actual speed of bar movement (dashed line), indicating that accurate readout of motion was possible with data from a single trial. For electrical stimulation, the strength of the motion signal as a function of putative stimulus speed was similar (Figure 3A, gray traces), indicating that electrically elicited signals carried roughly the same information about stimulus speed as visually elicited signals.

To compare quantitatively the fidelity of the real and artificial visual motion signals, the variability of speed estimates obtained from spike trains across trials was examined, for both visual and electrical stimulation. This quantity captures the precision of speed estimates that can be obtained from the spike trains in the recorded cells, a summary of motion sensing fidelity (Frechette et al., 2005). Speed estimate precision, indicated by the width of the distribution of speed estimates across trials, was similar for visually and electrically elicited spike trains, in three preparations (Figure 3B, black and gray histograms), and resembled results obtained across a range of visual stimulus speeds in previous work (Frechette et al., 2005). Thus, electrical stimulation elicited responses in ON parasol cells that carried similar behaviorally relevant information about visual motion as the visually elicited responses. Although other stimulus speeds were not tested, the high temporal precision of electrically elicited spikes would be expected to be particularly useful in conveying accurate estimates of speed for higher stimulus speeds.

DISCUSSION

Focal electrical stimulation reproduced the patterns of spiking elicited by moving stimuli, cell-by-cell and spike-by-spike, in complete local populations of ON parasol ganglion cells in the primate retina. The electrically induced activity exhibited higher temporal precision than light-evoked activity and produced a representation of motion with a fidelity comparable to that of the normal visual signal.

Although the combination of cell-type specificity, spatial and temporal precision, and completeness of electrically elicited activity exceeded the scope of previous work (Nirenberg and Pandarinath, 2012; Jensen et al., 2009; Hottowy et al., 2012; Fried et al., 2006; Ryu et al., 2011), additional work would be required to fully understand the generality and impact of these findings for future epiretinal prostheses, for several reasons.

(1) Although focal activation of individual cells is clearly possible among the dominant RGC types in the primate retina (Sekirnjak et al., 2008; Jepson et al., 2013), and was achieved here in small collections of ON parasol cells, the reliability of activation of one cell without activation of any cells of other types has yet to be fully documented. This issue is particularly serious in more central retina where cell density is higher and near the fovea where RGCs form several cell layers. In addition, the spatial extent of the stimulation region will play a major role in useful artificial vision.

(2) In a prosthesis, identification of cell types for stimulation could potentially be accomplished by recording with the electrodes of the device, but in a blind patient the accompanying light stimulation would not be possible. Thus, cell

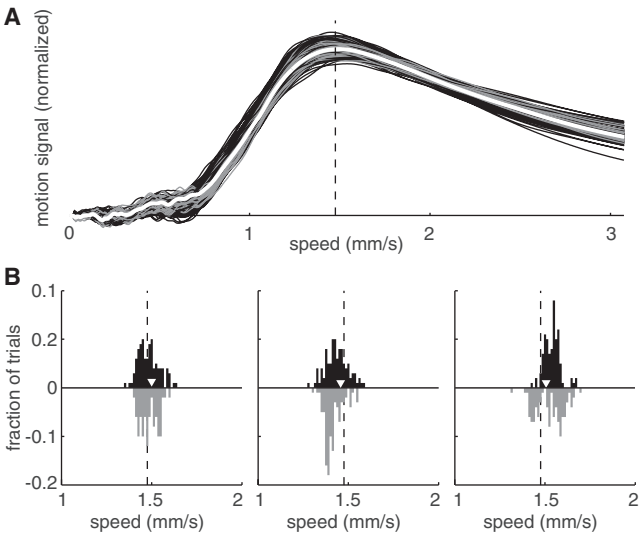

Figure 3. Inferring Stimulus Speed from Recorded Spike Trains

A motion-decoding algorithm (Frechette et al., 2005) based on known features of motion sensing in the primate visual system was used to infer the speed of the moving stimulus from recorded spike trains. This decoding was performed by computing the strength of a motion signal as a function of putative stimulus speed and then identifying the speed that yielded the strongest motion signal. (A) For each recorded trial of visual and electrical stimulation (100 or 50 trials, respectively), the strength of the motion signal extracted from retinal spike trains is shown as a function of putative speed. Vertical line indicates true speed of the visual stimulus. Each black curve was obtained from a single trial of visual stimulation, each gray curve from a single trial of electrical stimulation, from the same six cells as Figures 1 and 2. The white curve represents data from the visual stimulus trial selected for reproduction with electrical stimulation. (B) Variability of speed estimates for visual and electrical stimulation. Histograms in the left panel indicate the speed estimates obtained by identifying the peaks of the curves shown in (A). Top (black) histogram indicates estimates from visual stimulation, bottom (gray) from electrical stimulation. White arrowheads indicate speed estimates of visual stimulus trials chosen for reproduction. Speed estimates were near the true stimulus speed for both kinds of stimulation. Two additional data sets are shown, in the middle (eight cells) and right (six cells) histograms, each with 100 trials of visual and electrical stimulation. In each case, the SDs of speed estimates obtained from visual stimulation (0.058, 0.063, and 0.044 mm/s across preparations) and electrical stimulation (0.050, 0.049, and 0.079 mm/s) were similar.

type identification would likely be based on intrinsic properties of the cells recorded, such as spike train temporal structure (Devries and Baylor, 1997; Field et al., 2007) and axon conduction velocity.

(3) The possibility of unwanted activation of axons must be tested with larger electrode arrays, particularly in light of elongated, arc-like phosphenes reported by epiretinal implant patients (J. Weiland, personal communication), as well as previous work on isolated retina (Jensen et al., 2005).

(4) Generalization across visual stimuli was not tested; for example, a range of speeds would be needed to yield useful artificial vision. Previous results (Frechette et al., 2005; Chichilnisky and Kalmar, 2002) indicate that similar patterns of activity are elicited by moving visual stimuli over a range of speeds and that the temporal resolution of electrically elicited spikes (~0.1 ms; Sekirnjak et al., 2008) is much finer than that of visual motion signals (~10 ms; Frechette et al., 2005), suggesting that the results will generalize. In a prosthesis, a visual encoding model for RGC populations would likely be used to determine the pattern of electrical stimulation (Pillow et al., 2008; Nirenberg and Pandarinath, 2012).

(5) Gaps in firing induced by visual stimulation were not reproduced by electrical stimulation; tackling this problem will require entirely different techniques. In the present conditions, the quality of the visual signal was not substantially affected (Figure 3B).

With these caveats, the present results suggest two principal conclusions. First, the spatial and temporal precision possible with epiretinal stimulation using high-density arrays of small electrodes, suggested by previous single-cell work (Sekirnjak et al., 2006; Sekirnjak et al., 2008; Jepson et al., 2013) (and see Jensen and Rizzo, 2006; Jensen et al., 2009), has the potential to be exploited to reproduce patterns of electrical activity in complete neural populations (Hottowy et al., 2012). This implies that at the spatial and temporal intervals tested, interactions between cells over space and time in response to electrical stimulation play a minimal role in shaping population responses. Furthermore, any subthreshold activation of nontargeted cells, which in principle could affect subsequent responses to electrical stimulation, had minimal impact on the behaviorally relevant visual signal. These observations are promising for the design of future high-resolution prostheses, because natural vision relies on the spatiotemporal patterns of activity transmitted from the retina to the brain. The net signal about visual movement communicated by electrically elicited retinal activity was precise enough to yield veridical estimates of stimulus speed based on current understanding of visual motion readout in the brain (Chichilnisky and Kalmar, 2003; Frechette et al., 2005; Adelson and Bergen, 1985; Simoncelli and Heeger, 1998). This suggests that behavioral motion sensing with a prosthesis could be as precise as with natural vision, at least with the ON parasol cells, at the retinal eccentricities tested.

Second, the high temporal precision of electrically elicited spikes relative to visually elicited spikes raises the possibility of focal patterned stimulation with temporal multiplexing, which could be important for prostheses directed at the central retina where RGC density is high. Specifically, recent work has shown that spatial patterns of current across multiple electrodes have the possibility of improving spatial resolution of stimulation, by targeting a single cell while minimizing activation of other cells (Jepson et al., 2014). However, developing tailored stimulation patterns optimized for stimulating multiple cells simultaneously is likely to be complex and constrained. Stimulating only one cell at each moment in time instead would greatly simplify the problem. Given that the temporal resolution of elicited spikes is much finer than that of visual responses in the conditions described here (Figure 3), an effective artificial neural code could be constructed by always stimulating cells asynchronously, producing a spatiotemporal pattern that in some cases differs from the normal pattern (which normally includes synchronous spikes), but by an amount that is lower than the intrinsic temporal variability of visual responses and thus is presumably

insignificant for visual behavior. This reasoning relies on minimal disruption of the normal retinal code by the omission of synchronized spikes in nearby cells, a condition which has direct empirical support in the case of visual motion signals (Frechette et al., 2005) but should be tested with other stimuli. If this time-multiplexing strategy is viable, it has the potential to significantly extend the range of conditions in which artificial vision with a retinal prosthesis can subserve naturalistic visual behavior.

EXPERIMENTAL PROCEDURES

Multielectrode recording and electrical and visual stimulation were performed in a preparation of isolated primate retina as described previously (Chichilnisky and Kalmar, 2002; Field et al., 2007; Sekirnjak et al., 2008; Jepson et al., 2013). Briefly, the eyes of terminally anesthetized macaque monkeys (*Macaca sp.*, male or female) were removed and immediately hemisected in room light. After removing the anterior portion of the eye and the vitreous humor, the posterior portion of the eye was maintained in darkness in oxygenated bicarbonate-buffered Ames solution (Sigma). Under infrared illumination, patches of intact retina were isolated and held RGC-side down on a custom multielectrode array (MEA). The retina was superfused with Ames solution at ~33°C. Data were collected from three preparations at temporal equivalent eccentricities of 34°, 41°, and 46° (Drasdo and Fowler, 1974; Chichilnisky and Kalmar, 2002).

A custom 64-channel multichannel electrical stimulation system (Hottowy et al., 2008, 2012) was used in conjunction with electrode arrays to electrically stimulate and record. The arrays consisted of 61 approximately hexagonally packed indium tin oxide electrodes (60 μm spacing) on a glass substrate, electroplated with platinum black (Litke, 1998; Sekirnjak et al., 2006; Jepson et al., 2013). Recordings were band-pass filtered between 43 and 5,000 Hz (–3 dB) and were amplified and digitized at 20 kHz for offline analysis. Spike waveforms recorded during visual stimulation were detected and clustered into groups of spikes generated by individual RGCs (Litke et al., 2004).

Visual stimuli were displayed on a cathode ray tube computer monitor, optically reduced, and focused through a microscope objective onto the photoreceptor outer segments (Chichilnisky and Kalmar, 2002). The stimulus was maintained at low photopic intensity with neutral density filters. A spatiotemporal white noise stimulus was used to measure light response properties of RGCs (Chichilnisky, 2001). Functionally distinct RGC types were identified based on visual response properties, electrical properties, and density (Chichilnisky and Kalmar, 2002; Field et al., 2007). Receptive fields of cells (Figure 1) were summarized with the 1 SD boundary of an elliptical Gaussian fit to the spatial sensitivity profile obtained from the spike-triggered average stimulus during spatiotemporal noise stimulation (Chichilnisky and Kalmar, 2002).

Current pulses (150–300 μs total duration, triphasic, charge balanced [Hottowy et al., 2012; Jepson et al., 2013]) were injected with custom circuitry that permitted independent timing control on each electrode, as well as artifact reduction for recording and stimulating from the same electrode (Hottowy et al., 2008). Spikes recorded during electrical stimulation were analyzed with custom semiautomated procedures (Jepson et al., 2013). Briefly, recorded waveforms consisting of a mixture of spikes and electrical artifact were segregated automatically, then inspected for errors and manually corrected when necessary. Elicited spikes were consistent with direct activation of RGCs, based on the observed submillisecond response latency (Sekirnjak et al., 2006; Sekirnjak et al., 2008; Jepson et al., 2013).

ON parasol cells were selected for replication of visual responses with electrical stimulation. An initial scan was performed in which ON parasol cell responses to electrical stimulation were first measured for every electrode separately. The initial scan was used to identify a set of amplitudes required to elicit responses with probability ~0.9–1.0 in each cell. Moving bar stimuli (width 0.90°, speed 6.71 deg/s, 96% incremental contrast) were presented drifting across a uniform field of the same mean intensity as the spatiotemporal noise stimulus (see above). A single trial of the recorded responses to the moving bar visual stimulus was then selected to be reproduced with electrical stimulation. The trial was selected to minimize the summed difference between the spike trains recorded on that trial and spike trains recorded on all other trials, based on a spike distance metric (Victor and Purpura, 1997) normalized by the number of spikes. The timing of the current pulses for electrical stimulation was given by the timing of the spikes recorded in the selected visual stimulus trial, rounded to the nearest millisecond. The amplitudes of current pulses were varied systematically over a range of ~0.5–1.5 times the amplitudes identified in the initial scan, while keeping the current amplitudes on different electrodes in a fixed ratio. Data in Figures 2 and 3 were obtained with a set of stimulus amplitudes that yielded consistent activation across cells while minimizing current amplitude and resulting electrical artifacts and activation of nontargeted cells. Recorded responses to the electrical stimulation pattern were then compared to those elicited by the visual stimulus.

ACKNOWLEDGMENTS

This work was supported by the following: NEI grant EY021271 (E.J.C.), NSF grant PHY-0750525, NIH Grant EB004410, and the McKnight Foundation (A.M.L.), the Polish Ministry of Science and Higher Education and its grants for Scientific Research (W.D.), Polish National Science Centre grant DEC-2013/10/M/NZ4/00268 (P.H.), and San Diego Foundation Blasker Award (G.A.W.). We thank Martin Greschner and Clare Hulse for assistance during experiments, Marvin Thielk for analysis software development, E. Callway, J. Reynolds, and T. Albright for access to retinas, and Devon Sandel for analysis assistance.

Accepted: April 23, 2014
Published: June 5, 2014

REFERENCES

Adelson, E.H., and Bergen, J.R. (1985). Spatiotemporal energy models for the perception of motion. J. Opt. Soc. Am. A *2*, 284–299.

Barry, M.P., and Dagnelie, G.; Argus II Study Group (2012). Use of the Argus II retinal prosthesis to improve visual guidance of fine hand movements. Invest. Ophthalmol. Vis. Sci. *53*, 5095–5101.

Chichilnisky, E.J. (2001). A simple white noise analysis of neuronal light responses. Network *12*, 199–213.

Chichilnisky, E.J., and Kalmar, R.S. (2002). Functional asymmetries in ON and OFF ganglion cells of primate retina. J. Neurosci. *22*, 2737–2747.

Chichilnisky, E.J., and Kalmar, R.S. (2003). Temporal resolution of ensemble visual motion signals in primate retina. J. Neurosci. *23*, 6681–6689.

da Cruz, L., Coley, B.F., Dorn, J., Merlini, F., Filley, E., Christopher, P., Chen, F.K., Wuyyuru, V., Sahel, J., Stanga, P., et al.; Argus II Study Group (2013). The Argus II epiretinal prosthesis system allows letter and word reading and long-term function in patients with profound vision loss. Br. J. Ophthalmol. *97*, 632–636.

Dacey, D.M. (2004). Origins of perception: retinal ganglion cell diversity and the creation of parallel visual pathways. In The Cognitive Neurosciences, M.S. Gazzaniga, ed. (Cambridge: MIT Press), pp. 281–301.

Dacey, D.M., and Petersen, M.R. (1992). Dendritic field size and morphology of midget and parasol ganglion cells of the human retina. Proc. Natl. Acad. Sci. USA *89*, 9666–9670.

Devries, S.H., and Baylor, D.A. (1997). Mosaic arrangement of ganglion cell receptive fields in rabbit retina. J. Neurophysiol. *78*, 2048–2060.

Dorn, J.D., Ahuja, A.K., Caspi, A., da Cruz, L., Dagnelie, G., Sahel, J.A., Greenberg, R.J., and McMahon, M.J.; gus II Study Group (2013). The detection of motion by blind subjects with the epiretinal 60-electrode (argus II) retinal prosthesis. JAMA Ophthalmol. *131*, 183–189.

Drasdo, N., and Fowler, C.W. (1974). Non-linear projection of the retinal image in a wide-angle schematic eye. Br. J. Ophthalmol. *58*, 709–714.

Field, G.D., Sher, A., Gauthier, J.L., Greschner, M., Shlens, J., Litke, A.M., and Chichilnisky, E.J. (2007). Spatial properties and functional organization of small bistratified ganglion cells in primate retina. J. Neurosci. *27*, 13261–13272.

Frechette, E.S., Sher, A., Grivich, M.I., Petrusca, D., Litke, A.M., and Chichilnisky, E.J. (2005). Fidelity of the ensemble code for visual motion in primate retina. J. Neurophysiol. *94*, 119–135.

Fried, S.I., Hsueh, H.A., and Werblin, F.S. (2006). A method for generating precise temporal patterns of retinal spiking using prosthetic stimulation. J. Neurophysiol. *95*, 970–978.

Hottowy, P., Dąbrowski, W., Skoczeń, A., and Wiącek, P. (2008). An integrated multichannel waveform generator for large-scale spatio-temporal stimulation of neural tissue. Analog. Integr. Circ. Sig. Process *55*, 239–248.

Hottowy, P., Skoczeń, A., Gunning, D.E., Kachiguine, S., Mathieson, K., Sher, A., Wiącek, P., Litke, A.M., and Dąbrowski, W. (2012). Properties and application of a multichannel integrated circuit for low-artifact, patterned electrical stimulation of neural tissue. J. Neural Eng. *9*, 066005.

Humayun, M.S., Dorn, J.D., da Cruz, L., Dagnelie, G., Sahel, J.A., Stanga, P.E., Cideciyan, A.V., Duncan, J.L., Eliott, D., Filley, E., et al.; Argus II Study Group (2012). Interim results from the international trial of Second Sight's visual prosthesis. Ophthalmology *119*, 779–788.

Jensen, R.J., and Rizzo, J.F., 3rd. (2006). Thresholds for activation of rabbit retinal ganglion cells with a subretinal electrode. Exp. Eye Res. *83*, 367–373.

Jensen, R.J., Ziv, O.R., and Rizzo, J.F., 3rd. (2005). Thresholds for activation of rabbit retinal ganglion cells with relatively large, extracellular microelectrodes. Invest. Ophthalmol. Vis. Sci. *46*, 1486–1496.

Jensen, R.J., Ziv, O.R., Rizzo, J.F., 3rd, Scribner, D., and Johnson, L. (2009). Spatiotemporal aspects of pulsed electrical stimuli on the responses of rabbit retinal ganglion cells. Exp. Eye Res. *89*, 972–979.

Jepson, L.H., Hottowy, P., Mathieson, K., Gunning, D.E., Dabrowski, W., Litke, A.M., and Chichilnisky, E.J. (2013). Focal electrical stimulation of major ganglion cell types in the primate retina for the design of visual prostheses. J. Neurosci. *33*, 7194–7205.

Jepson, L.H., Hottowy, P., Mathieson, K., Gunning, D.E., Dabrowski, W., Litke, A.M., and Chichilnisky, E.J. (2014). Spatially patterned electrical stimulation to enhance resolution of retinal prostheses. J. Neurosci. *34*, 4871–4881.

Klauke, S., Goertz, M., Rein, S., Hoehl, D., Thomas, U., Eckhorn, R., Bremmer, F., and Wachtler, T. (2011). Stimulation with a wireless intraocular epiretinal implant elicits visual percepts in blind humans. Invest. Ophthalmol. Vis. Sci. *52*, 449–455.

Litke, A.M. (1998). The retinal readout system: an application of microstrip detector technology to neurobiology. Nucl. Instrum. Methods Phys. Res. A *418*, 203–209.

Litke, A.M., Bezayiff, N., Chichilnisky, E.J., Cunningham, W., Dabrowski, W., Grillo, A.A., Grivich, M., Grybos, P., Hottowy, P., Kachiguine, S., et al. (2004). What does the eye tell the brain?: Development of a system for the large-scale recording of retinal output activity. IEEE Transactions on Nuclear Science *51*, 1434–1440.

Merigan, W.H., and Maunsell, J.H. (1990). Macaque vision after magnocellular lateral geniculate lesions. Vis. Neurosci. *5*, 347–352.

Nirenberg, S., and Pandarinath, C. (2012). Retinal prosthetic strategy with the capacity to restore normal vision. Proc. Natl. Acad. Sci. USA *109*, 15012–15017.

Perry, V.H., Oehler, R., and Cowey, A. (1984). Retinal ganglion cells that project to the dorsal lateral geniculate nucleus in the macaque monkey. Neuroscience *12*, 1101–1123.

Pillow, J.W., Shlens, J., Paninski, L., Sher, A., Litke, A.M., Chichilnisky, E.J., and Simoncelli, E.P. (2008). Spatio-temporal correlations and visual signalling in a complete neuronal population. Nature *454*, 995–999.

Ryu, S.B., Ye, J.H., Goo, Y.S., Kim, C.H., and Kim, K.H. (2011). Decoding of temporal visual information from electrically evoked retinal ganglion cell activities in photoreceptor-degenerated retinas. Invest. Ophthalmol. Vis. Sci. *52*, 6271–6278.

Sekirnjak, C., Hottowy, P., Sher, A., Dabrowski, W., Litke, A.M., and Chichilnisky, E.J. (2006). Electrical stimulation of mammalian retinal ganglion cells with multielectrode arrays. J. Neurophysiol. *95*, 3311–3327.

Sekirnjak, C., Hottowy, P., Sher, A., Dabrowski, W., Litke, A.M., and Chichilnisky, E.J. (2008). High-resolution electrical stimulation of primate retina for epiretinal implant design. J. Neurosci. *28*, 4446–4456.

Shepherd, R.K., Shivdasani, M.N., Nayagam, D.A., Williams, C.E., and Blamey, P.J. (2013). Visual prostheses for the blind. Trends Biotechnol. *31*, 562–571.

Simoncelli, E.P., and Heeger, D.J. (1998). A model of neuronal responses in visual area MT. Vision Res. *38*, 743–761.

Victor, J.D., and Purpura, K.P. (1997). Metric-space analysis of spike trains: theory, algorithms and application. Network *8*, 127–164.